Geometric Brain Signatures for Diagnosing Rare Hereditary Ataxias and Predicting Function

Zuitian Tao PhD[a], Gilles Naejie PhD[b], Fuad Noman PhD[c], Thiago J R Rezende PhD[d], Marcondes Franca PhD[d], Alex Fornito PhD[a], Ian H Harding PhD[e,f], Nellie Georgiou-Karistianis PhD[a], Trang Cao PhD[a†], Susmita Saha PhD[a,f†]; TRACK-FA Neuroimaging Consortium[‡]

a School of Psychological Sciences, The Turner Institute for Brain and Mental Health, Monash University, Clayton, Australia.
b Laboratoire de Cartographie fonctionnelle du Cerveau (LCFC), UNI - ULB Neuroscience Institute, Université libre de Bruxelles (ULB), 808 Lennik Street, 1070, Brussels, Belgium.
c School of Information Technology, Monash University Malaysia, Subang Jaya, Malaysia
d Department of Neurosciences, School of Medicine, University of São Paulo at Ribeirão Preto (USP-RP), Ribeirão Preto, SP, Brazil.
e QIMR Berghofer Medical Research Institute, Brisbane, Australia.
f School of Translational Medicine, Monash University, Melbourne, Australia.

† Co-Senior authors
‡ see Acknowledgments for collaborators

Corresponding author
Dr. Susmita Saha
School of Psychological Sciences,
The Turner Institute for Brain and Mental Health,
Monash University, Clayton, Australia.
Email: saha.saha@monash.edu
T: +61 3 990 24701

Key Points

Question

Can geometric brain signatures derived from routine structural MRI enable accurate diagnosis of hereditary cerebellar ataxia subtypes, track disease progression and predict function?

Findings

Using a combined geometric and machine-learning framework, we identified cortical geometric signatures that served as generalisable biomarkers for differential diagnosis across hereditary ataxia subtypes. Functional-MRI-equivalent signatures were predicted from structural MRI in both health and disease. Structural and predicted functional biomarkers showed greater sensitivity to annual disease progression than conventional volumetric measures.

Meaning

Structural MRI may provide scalable, objective geometric biomarkers for diagnostic decision support, guiding targeted genetic testing, disease monitoring, and functional inference.

Abstract

Importance

Hereditary cerebellar ataxias (HCAs) are rare neurodegenerative disorders characterised by progressive motor impairment and overlapping clinical phenotypes. Although genetic testing provides etiological diagnosis, diagnostic delays frequently arise before targeted testing, owing to non-specific presentation and limited clinician familiarity. Imaging-derived biomarkers that capture phenotypic expression and network-level consequences of disease could support earlier recognition of hereditary ataxia, guide appropriate genetic testing, and provide sensitive measures of disease evolution.

Objective

Building on evidence that cortical geometry shapes functional organisation, we hypothesised that geometric signatures derived from structural magnetic resonance imaging (sMRI) could discriminate HCA subtypes and yield progression-sensitive biomarkers, while enabling scalable prediction of function.

Design, Setting, and Participants

We decomposed sMRI and task-evoked functional MRI data from three independent cohorts using cortical geometric eigenmodes, intrinsic spatial patterns defined by cortical surface geometry, to obtain structural and functional geometric signatures. Structural signatures were used to train neural networks for disease classification and to derive biomarkers sensitive to annual progression. We further modelled structure-to-function mappings to predict functional geometric signatures from sMRI and evaluated their diagnostic and longitudinal utility.

Main Outcomes and Measures

Diagnostic performance assessed using area under the curve (AUC), accuracy, precision, recall, and F1 score; accuracy of structure-to-function prediction assessed using coefficient of determination (R^2) and correlation between predicted and empirical activation maps; and sensitivity to disease progression assessed using longitudinal effect sizes (Cohen's d).

Results

Our framework achieved high diagnostic performance, distinguishing healthy controls from Friedreich ataxia (FRDA) with a maximum AUC of 0.93 and separating FRDA from spinocerebellar ataxia type 1 (SCA1) and SCA3, with AUCs up to 0.81, showing cross-cohort generalisability. Structure-to-function-signature prediction achieved R^2 up to 0.62 and correlation reaching 0.86 across health and disease, while predicted functional signatures improved classification beyond structural signatures alone and enabled

partial reconstruction of individual task-activation map. Geometric brain signatures showed greater progression sensitivity than conventional volumetric MRI measures.

Conclusions and Relevance

This geometry-driven framework offers novel, objective, multiscale biomarkers for diagnostic-decision-support and monitoring HCAs and provides proof-of-concept for the feasibility of predicting fMRI-equivalent biomarkers in disease from routine sMRI, which is far more practical in movement-disorder populations.

Introduction

Hereditary cerebellar ataxias (HCAs) are rare, progressive neurodegenerative movement disorders characterised by heterogeneous motor and non-motor symptoms, wide variability in age of onset, and diverse trajectories of functional decline.[1–4] Although current genetic diagnostics, particularly repeat-expansion assays and targeted panels, provide efficient and reliable etiological confirmation for common HCAs, patients frequently experience prolonged diagnostic pathways. In clinical practice, these delays arise from phenotypic overlap between ataxia symptoms, variable referral pathways, limited clinician familiarity and limited genetic test access.[5–9] In this context, tools that support early phenotypic characterisation may help clinicians recognise when a particular HCA subtype is likely, guide timely and targeted genetic investigations, and ultimately shorten the path to definitive diagnosis.

Even after genetic diagnosis is established, major bottlenecks remain in monitoring disease evolution.[10–13] HCAs are increasingly understood as disorders of distributed cerebro-cerebellar systems, in which primary pathology in the cerebellum and its afferent/efferent connections can have widespread downstream consequences for cortical organisation and large-scale networks.[14] This systems-level perspective motivates the search for biomarkers that capture phenotypic expression and network-level consequences of disease signals that are not available from genotype alone.

Current outcome assessment in natural history studies and clinical trials relies largely on clinical rating scales such as the Scale for the Assessment and Rating of Ataxia (SARA) and the modified Friedreich Ataxia Rating Scale (mFARS), which are sensitive to clinically meaningful change, however, remain subjective, rater-dependent, less sensitive in later disease stages (e.g., reduced responsiveness in non-ambulatory FRDA patients) and provide only coarse summaries of complex neurobiological processes.[1,11,13,15–17] On the other hand, structural magnetic resonance imaging (sMRI) offers a more objective alternative,[13] consistently demonstrating progressive cerebellar and brainstem atrophy across HCA subtypes, with distinct and variable involvement of cerebral regions. For example, spinocerebellar ataxia type 1 (SCA1) is characterised by early pontine and cerebellar degeneration frequently accompanied by cortical thinning and frontal and parietal atrophy;[10,18] SCA3 shows widespread cerebellar and brainstem involvement with milder supratentorial changes emerging later in the disease course;[19] and FRDA follows a distinct pattern marked by dentate nucleus atrophy, spinal cord thinning, and degeneration of the superior cerebellar peduncles and corticospinal tracts, with limited late-stage supratentorial involvement.[20,21] Although such signatures inform clinical reasoning, automated and generalisable imaging-based diagnostic models in HCAs remain limited.[22–24] Existing studies are frequently single-site, underpowered, focused on narrow classifications, or reliant on local voxel/vertex/ROI analyses that can be sensitive to analytic choices and reduce reproducibility.[25] In addition, conventional sMRI measures have shown limited sensitivity to longitudinal changes.[26,27] Objective, reproducible biomarkers derived from a widely available imaging modality (e.g. sMRI) that enable earlier diagnostic decision support and more sensitive progression monitoring are therefore urgently needed.

Functional MRI (fMRI) has provided important insights into network-level dysfunction in FRDA and SCAs, including altered cortical activation and connectivity patterns that complement structural findings.[28,29] However, fMRI remains challenging to acquire in movement-disorder populations because of motion artefacts, task-compliance demands, and variability, which has limited both research use and

clinical translation.[13,30] Approaches capable of inferring functional signatures from more accessible modalities such as sMRI could help overcome these barriers. To date, only one deep-learning (DL) study has attempted structure-to-function prediction in healthy individuals, but it reported only indirect evidence of individual-level correspondence (comparison of self-vs-other correlations) without providing any quantitative accuracy of predicted task-activation maps.[31] Disease-specific investigations, therefore remain lacking.

To address these clinical and translational challenges in HCAs, we sought an imaging representation that is anatomically grounded yet sensitive to multiscale network organisation, interpretable, scalable, and reproducible across sites, and naturally suited to linking structure and function. Cortical geometric eigenmodes provide such a representation. They are intrinsic spatial patterns determined by the geometry of the cortical surface, and their ordered, multiscale structure, from coarse, low-frequency modes to fine, high-frequency modes, allows simultaneous sensitivity to widespread network abnormalities and more localised cortical changes.[32] Recent work shows that any individual cortical map, whether structural or functional, can be expressed as a weighted combination of these modes, each with a characteristic spatial fingerprint.[33–35] This enhances reproducibility and reduces dependence on analytic choices, while the associated mode weights serve as personalised structural or functional geometric signatures. Finally, because structural and functional maps share the same geometric constraint, eigenmodes provide a natural bridge between anatomy and function.[33,34]

In this study, we developed and validated a geometry-driven DL framework that used cortical eigenmodes to (i) derive multiscale, interpretable sMRI biomarkers and evaluate their performance for differential classification across major HCA subtypes (with FRDA as the primary case study and comparisons including SCA1 and SCA3); (ii) model structure-to-function mappings to predict fMRI-equivalent functional signatures from sMRI alone, providing scalable access to functional signatures when fMRI is unavailable; and (iii) assess the sensitivity of structural and predicted functional

geometric signatures to longitudinal change, benchmarking against clinical and volumetric MRI measures.

Methods

We developed diagnosis and prediction models by integrating eigenmode decomposition with DL approaches and using sMRI and task-fMRI data from participants across three independent cohorts: the Belgium dataset,[36] the TRACK-FA dataset,[37] and the Campinas dataset[38–40] (see Supplementary Tables S1, S2, and S3 for demographic details). Figure 1 presents an overview of the workflow. Detailed descriptions of participants, MRI acquisition protocols, preprocessing, eigenmode derivations, feature selection, model architectures, training, evaluation, performance analysis[41] and methodological justifications are provided in the Supplementary Methods.

HCA Diagnosis With Structural Geometric Features

To develop the HCA diagnosis model, cortical thickness maps of each hemisphere, derived from T1-weighted MRIs, from the Belgium dataset (21 healthy controls (HCs), 20 FRDA) were decomposed using 200 geometric eigenmodes to obtain the β-weight of each mode. As the brain is asymmetric,[42] our models consider each hemisphere separately in order to identify hemisphere-specific signatures. Feature selection and evaluation of the DL diagnosis model were nested within a leave-one-out cross-validation framework. Within each training fold, mode-specific β-weights were compared between groups using two-sample *t*-tests (uncorrected $p < 0.05$). Justification for the use of uncorrected statistical significance is provided in Supplementary Methods 5. Significantly different β-weights, i.e., structural geometric signatures, constitute the structural input features into a fully connected neural-network classifier for FRDA versus HC diagnosis (Supplementary Methods 6.1). Cross-cohort generalisability was evaluated via transfer learning in the larger, independent, multi-site TRACK-FA cohort (n=168 FRDA; n=92 HCs) (Supplementary Methods 6.3). For differential diagnosis among HCA subtypes, separate models were trained to classify FRDA vs SCA1, FRDA vs SCA3, and SCA1 vs SCA3 using the Campinas dataset,

with five-fold cross-validation. We then benchmarked our models using geometric features with a model using conventional features derived from principal component analysis (PCA) of the CT maps from Belgium dataset (Supplementary Methods 7). Model performance was evaluated using AUC, accuracy, precision, recall, and F1-score, with AUC considered as the primary metric for model comparison.

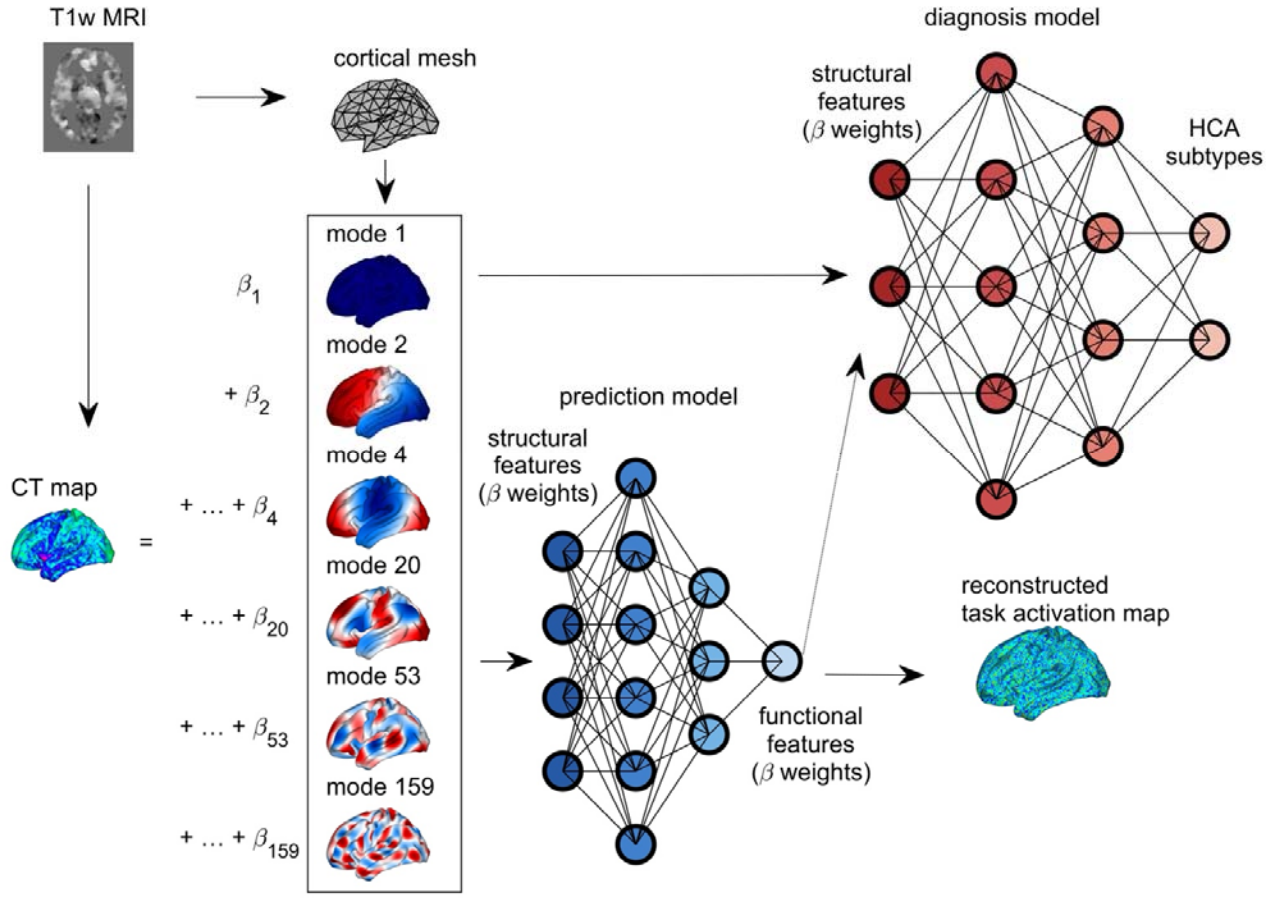

Figure 1. **Overview of the geometry-driven DL framework linking cortical structure to functional activation and diagnosis**. A set of geometric eigenmodes are derived from the population-averaged cortical surface mesh obtained from T1-weighted (T1w) MRI. Individual cortical thickness maps extracted from T1w MRI are decomposed as weighted linear combinations of these modes ($\beta_1 \ldots \beta_{200}$) and the resulting eigenmode weights constitute the structural features. Task-evoked fMRI activation maps from the passive-movement task are decomposed in the same way, with their eigenmode weights serving as functional features. Selected structural features are input into a neural-network prediction model to predict functional features, which are then used to reconstruct individual task-activation maps. In parallel, selected structural, empirical functional and/or predicted functional features are provided to neural network diagnosis models to generate diagnostic labels (HCA subtypes).

HCA Diagnosis With Functional Geometric Features

In addition to structural MRI-based diagnosis, we hypothesised that task-based fMRI could further improve diagnostic performance. Accordingly, functional activation maps from passive-movement-evoked fMRI in the Belgium dataset were decomposed using geometric eigenmodes to obtain mode β-weights. Functional features were selected from statistical test similar to structural features and used alone or combined with structural features for the diagnostic models, following the same training and cross-validation strategy (Supplementary Methods 6.1). Benchmarking was also performed using PCA-based models.

Prediction Of Functional Geometric Features Solely From Structural Geometric Features

Because fMRI acquisition is often impractical in ataxia cohorts, we trained neural network regression models to predict functional geometric signatures (β weights of fMRI task activation maps), solely from structural geometric signatures (β weights of cortical thickness maps). We used both HCs and FRDA patients' data from the Belgium cohort. Model training, feature selection, and evaluation procedures are detailed in Supplementary Methods 6.2. Predicted functional β weights were also used to reconstruct task activation maps, with reconstruction accuracy quantified as the correlation between empirical and reconstructed maps (Supplementary Methods 4.2). PCA based models were included for benchmarking.

Diagnostic Utility Of Predicted Functional Geometric Features

Structure to function prediction models trained on the Belgium dataset were applied to TRACK FA structural MRI to generate predicted functional features (Supplementary Methods 6.2). These predicted features were then used to fine tune the Belgium trained diagnostic models, whether originally based on functional features alone or on combined structural and functional features, via transfer learning, enabling assessment of their added diagnostic utility and cross cohort robustness.

Sensitivity of Geometric Features to Disease Progression

We quantified disease progression sensitivity in TRACK FA by calculating effect sizes (Cohen's *d)* for each structural and functional geometric feature between baseline and 1 year follow up (Supplementary

Methods 8). Features were considered sensitive if the longitudinal changes met these criteria: (i) exhibiting opposite directions of change between the HCs and FRDA groups, (ii) between-group difference in effect size exceeding $|\Delta d| > 0.3$ and (iii) statistically significant (two-sample t-tests, $p < 0.05$; uncorrected) (Supplementary Methods 8).

Linking Eigenmodes to Functional Networks

The mapping of eigenmodes to functional networks, used to aid interpretability, is detailed in Supplementary Methods 9.

Results

HCA Diagnosis With Structural Geometric Features

We analysed structural geometric features, i.e., β-weights quantifying how strongly individual's CT map expresses the spatial pattern of each eigenmode. Several eigenmodes showed significant group differences (two-sample t-test, $p < 0.05$) in β-weights between HCs and FRDA patients in the Belgium cohort (Figure 2a and b). These findings indicate both widespread large-scale disruptions and more spatially localised changes in FRDA, spanning across three canonical frequency bands: low (modes 1-50, wavelength ~60 mm)), mid (51-100, ~40 mm), and high-frequency (101-200, ~30 mm). Modes with significant β-differences are listed in Supplementary Table S4. Note that modes 2, 4, 20, 41, 53, and 159 showed significant β-differences in both hemispheres, suggesting consistent bilateral alterations in thickness patterns. Mapping the spatial expression of these modes onto canonical functional networks revealed that the dominant lobes of the altered eigenmodes preferentially overlapped limbic, somatomotor, and ventral attention/salience and frontoparietal control regions. This pattern suggests that cortical territories aligned with these networks are preferentially involved in the thickness alterations observed in FRDA.

Comprehensive diagnostic performance measures for all models are provided in Supplementary Tables S5-S6 and Figure 2c–d. The HC-FRDA diagnostic model trained on structural geometric features achieved strong performance in both hemispheres (AUC: 0.88 left, 0.85 right), with comparable transfer-learning performance in the independent TRACK-FA cohort, where right hemisphere performance was marginally higher.

In differential diagnosis among HCA subtypes, classification performance varied across subtype comparisons. In particular, models distinguishing SCA1 vs FRDA achieved the highest performance (AUC: 0.81, right and AUC: 0.77, left) while the SCA1 vs SCA3 models exhibited the lowest (AUC: 0.53, left). Overall, these findings suggest that the weights associated with geometry-constrained, multiscale cortical thickness patterns constitute promising and potentially generalisable biomarkers for automated differential diagnosis of HCAs. However, distinguishing between closely related SCA subtypes remains challenging. The modes exhibiting significant β-differences for these models are listed in Supplementary Tables S7-9. These modes span both large-scale and localised patterns. In the FRDA versus SCA1 differentiating, modes 1, 4, and 9 showed bilateral significance, whereas in FRDA versus SCA3, modes 1, 4, and 108 were bilaterally altered. Spatially, dominant lobes of these modes align preferentially with limbic, somatomotor, and frontoparietal control territories in FRDA vs SCA1 differentiating, and with limbic and somatomotor territories in the FRDA vs SCA3 differentiating. Benchmarking outcomes from all PCA based diagnostic and prediction models are provided in the Supplementary Results 1.

HCA Diagnosis With Functional Geometric Features

Consistent with the structural findings, uncorrected significant group differences in eigenmode β weights derived from task-activation maps in Belgium data were observed in both hemispheres (Supplementary Table S10 and Figures S1) with modes 1, 4, 63, 99, and 122 altered bilaterally. These modes primarily overlapped limbic, somatomotor, attention, default mode, and visual networks. Spatial mapping analysis

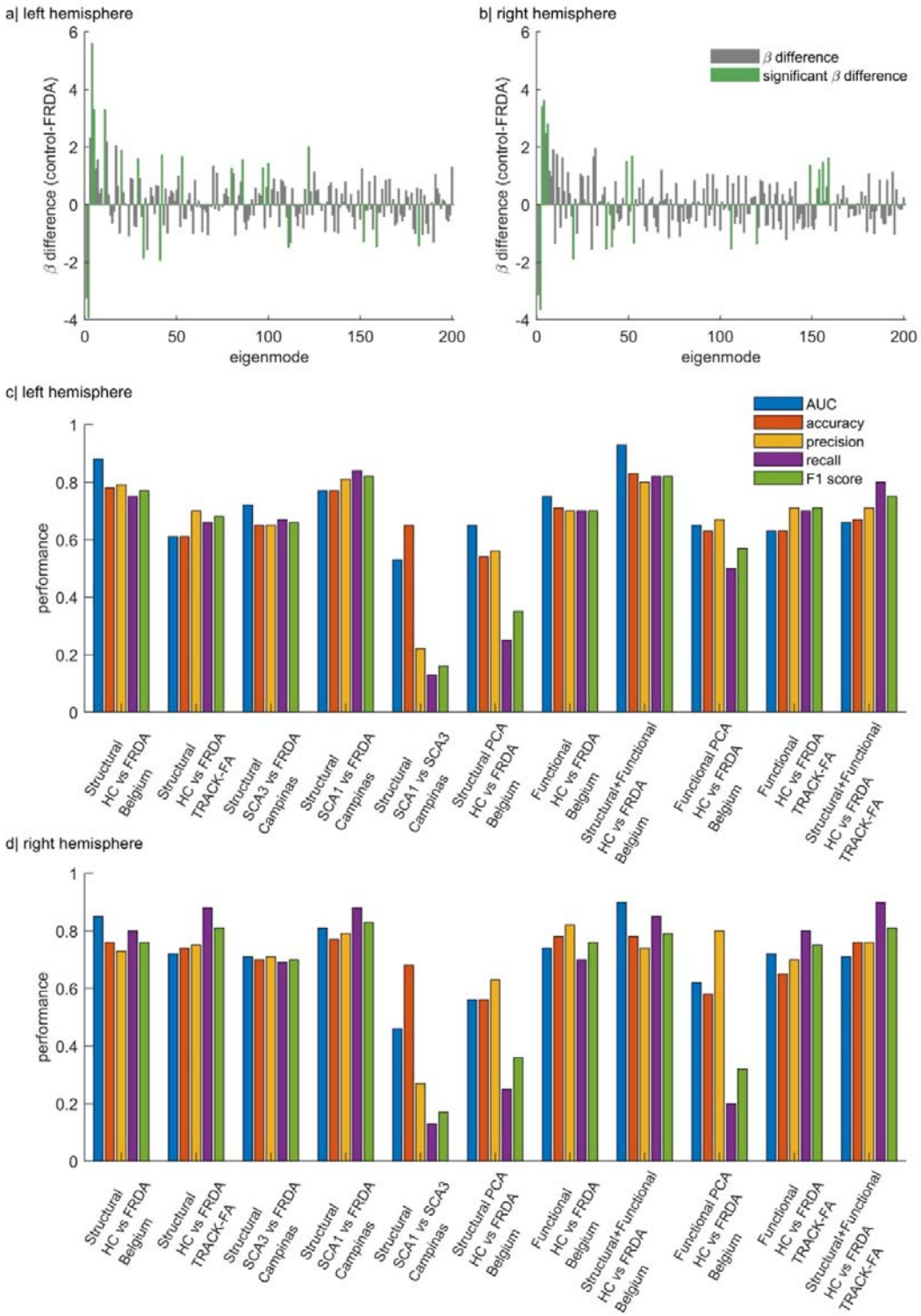

Figure 2. Illustration of diagnostic features and model performance. Differences in structural eigenmode weights between HCs and FRDA patients are shown for eigenmodes 1–200 in the a| left hemisphere and b| right hemisphere. Performance of diagnostic models using c| left hemisphere features and d| right hemisphere features is quantified using AUC, accuracy, precision, recall, and F1 score. Note that in the Belgium dataset, functional denotes features derived from empirical fMRI data, whereas in TRACK-FA, it refers to predicted functional features.

showed that the dominant regions expressing these altered modes overlapped primarily with limbic, somatomotor, dorsal and ventral attention, default mode, and visual networks. Diagnostic models using functional geometric features achieved performance (AUC: 0.75, left) (Figure 2c–d). Combining structural and functional features further improved diagnostic performance (AUC: 0.93, left), surpassing that of single-modality models. These results suggest that geometry-driven structural and functional features capture complementary disease-related information.

Prediction Of Functional Geometric Features Solely From Structural Geometric Features

To examine whether fMRI-equivalent features can be reliably predicted from sMRI alone, we trained 200 separate models, each predicting one functional geometric feature from the corresponding set of structural geometric features. Across models, prediction performance reached a mean R^2 of 0.26 ± 0.22 (range: -0.70 - 0.56) with a mean correlation of 0.68 ± 0.10 (range: 0.24 - 0.86) in the left hemisphere and R^2 of 0.24 ± 0.17 (-0.51 - 0.62) with a correlation of 0.63 ± 0.12 (range: 0.25 - 0.86) in the right hemisphere. Although the average explained variance was modest, the wide range of metrics indicates that specific functional features were predicted with relatively high accuracy, highlighting that structural MRI captures substantial information about particular aspects of functional organisation in both HCs and FRDA patients. Functional geometric features that achieved high predictive performance ($R^2 > 0.5$ and correlation > 0.7) are listed in Supplementary Table S11. Further analysis of structure-to-function mapping is detailed in the Supplementary Results 2.

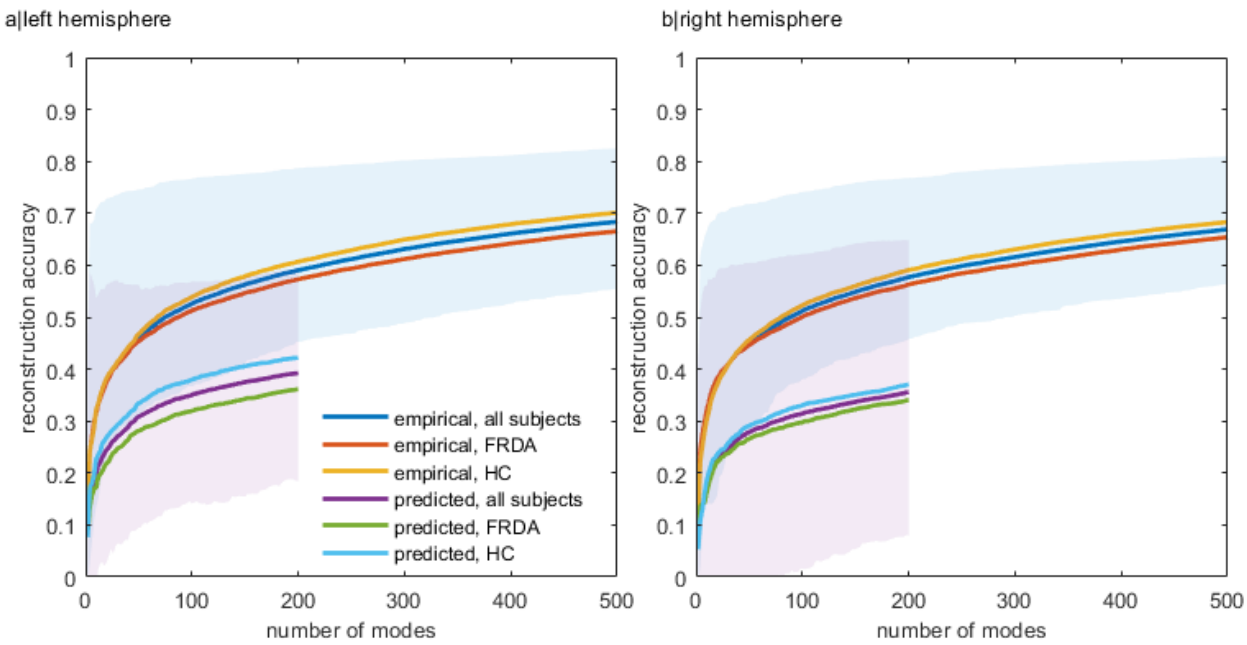

Figure 3. Reconstruction accuracy of task-activation maps using cortical eigenmodes.
Mean correlation between empirical and reconstructed individual task-activation maps in the Belgium dataset, using weights derived directly from empirical activation maps or predicted from structural features, as a function of the number of cortical eigenmodes for the a| left and b| right hemisphere. Results are shown separately for HCs, FRDA patients, and all subjects. Shaded regions indicate the range of reconstruction accuracy across individuals.

Using 200 empirical functional eigenmode weights, mean reconstruction accuracy across all subjects approached 0.6 in both hemispheres (range of correlations across individuals: 0.45-0.79, left; 0.46-0.77, right), indicating a moderate-to-strong correspondence between the reconstructed and empirical activation maps (Figure 3). This level of accuracy is comparable to prior work,[34] which reported >80% accuracy when using group-averaged rather than individual-level activation maps, as examined here. With predicted functional eigenmode weights, reconstruction accuracy remained moderate, with mean correlations of 0.39 (range: 0.19 - 0.60) in the left hemisphere and 0.36 (range: 0.08 - 0.65) in the right hemisphere across individuals, with slightly higher performance observed in HCs (see values for different cohorts in Supplementary Table S12). These findings highlight two key points: (i) eigenmode decomposition captures a substantial proportion of task-related variance in functional activation, and (ii) functional features predicted from structural features preserve meaningful information about individual brain activity patterns.

Diagnostic utility of predicted functional geometric features, evaluated in the independent TRACK-FA cohort using a transfer-learning framework, is reported in the Supplementary Results 3.

Sensitivity Of Geometric Features To Disease Progression

We next examined the sensitivity of geometric features to longitudinal disease progression in TRACK-FA, over a 1-year interval, using Cohen's *d* as an effect-size measure. Several structural geometric features (left: eigenmodes 23, 52, 57, 100, 116, 119, 144, and 179; right: eigenmodes 40, 69, 143, 153, 168, and 184 (Figure 4a, b), met our biomarker criteria (Supplementary Methods 8). These findings indicate that annual disease progression in FRDA predominantly affects mid- to high frequency eigenmodes, consistent with increasingly regional and localised structural alterations over time. This pattern contrasts with the broader low- and high-frequency alterations seen in HC-FRDA diagnostic models. Thus, while global-scale abnormalities define the disease signature at baseline, longitudinal progression appears to be driven by increasingly local disruptions, i.e., lower spatial scales. Spatial mapping showed that the progression-sensitive structural modes preferentially aligned with cortical territories spanning ventral attention/salience, default mode, visual, limbic, dorsal attention, and somatomotor networks, consistent with distributed cortical progression embedded within large-scale functional architectures.

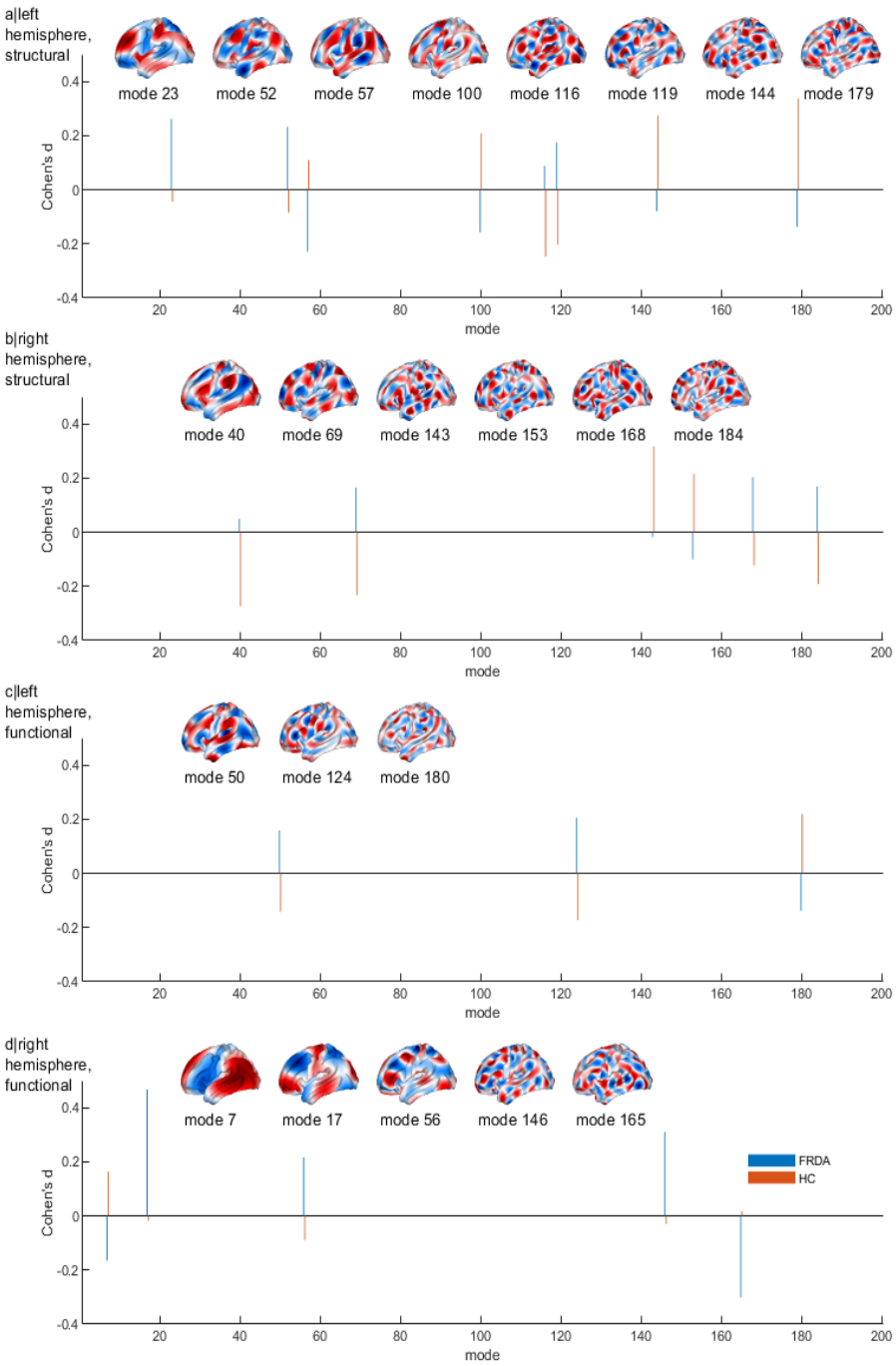

Figure 4. Geometric features sensitive to annual disease progression.
Geometric features showing opposite directional change over time, with absolute between-group differences in Cohen's greater than 0.3 ( ) and showing statistically significant (two□sample *t*□tests, $p < 0.05$; uncorrected) between-group differences, are presented alongside their corresponding values in HCs and FRDA patients. Panels a| and b| show structural geometric features in the left and right hemispheres, respectively, while panels c| and d| show predicted functional geometric features. Blue and orange vertical lines denote *d* values for HCs and FRDA patients, respectively.

With predicted functional features, progression-sensitive modes included eigenmodes 50, 124, and 180 in the left hemisphere (Figure 4c) and eigenmodes 7, 17, 56, 146, and 165 in the right (Figure 4d). These findings, together with spatial mapping, suggest hemispheric asymmetry in functional progression. Left-hemisphere modes aligned primarily aligned with limbic and dorsal attention territories, suggesting more localised disruption within these network-aligned regions. In contrast, right-hemisphere modes reflected both global low-frequency and local high-frequency alterations, with dominant involvement of default mode, dorsal and ventral attention, and frontoparietal control territomfarsries. In the left hemisphere, structural features generally exhibited greater sensitivity to progression than functional features, (peak: eigenmode 23; d in FRDA = 0.262). Conversely, in the right hemisphere, functional features were more sensitive than structural ones, with eigenmode 17 demonstrating the greatest sensitivity (d in FRDA = 0.467). Correlations between geometric features and clinical severity (mFARS) are reported in Supplementary Table S14.

For benchmarking, we computed Cohen's d for mFARS and conventional volumetric MRI measures (cerebellar volume and left/right superior cerebellar peduncle volume) in TRACK-FA. mFARS ($d = 0.53$) demonstrated sensitivity comparable to that of the top-performing predicted functional geometric feature. In contrast, volumetric measures were markedly less sensitive, with the largest effect size in FRDA reaching only $|d| = 0.11$ and all between-group effect size differences below 0.15. Overall, these results suggest that structural and predicted functional geometric features capture subtle longitudinal disease progression more effectively than traditional structural MRI biomarkers and may provide objective, complementary measures alongside clinical ratings.

Discussion

Our study provides proof-of-concept that cortical geometric eigenmodes, natural spatial patterns shaped by cortical geometry, encode subtype-specific signatures in HCAs. By leveraging geometric features derived from routine sMRI, our DL framework enabled differential diagnosis, prediction of fMRI-equivalent biomarkers, reliable approximation of individual task-activation patterns, and sensitive

monitoring of disease progression. These biomarkers complement conventional sMRI by capturing multiscale cortical organisation, from local to network-level structure, reveal functional network disruption from routine scans, and are far more practical in movement disorder populations. Additionally, empirical functional geometric features further improved diagnostic precision, and structure-predicted functional biomarkers enhanced both diagnostic accuracy and sensitivity to longitudinal change. This framework establishes a scalable pathway to augment phenotypic characterisation, guide targeted genetic testing and reduce diagnostic delay. Both structural and predicted functional geometric biomarkers provide objective, rater-independent measures of disease evolution that are more sensitive than conventional volumetric MRI features and demonstrate sensitivity comparable to established clinical rating scales.

Currently, MRI is primarily used as a complementary tool in a structured, rule-based, and semi-automated manner to guide differential diagnosis and support genetic testing.[44,45] Existing structural MRI-based automated diagnostic studies in HCAs are scarce, with only a few reporting accuracies comparable to ours, though based on very small cohorts.[24,46] Similarly, patient-control classification approaches for SCAs reported high accuracy, yet relied on small, single-site cohorts, lacked generalisability or external validation, and offered limited interpretability of features.[22,47] In contrast, our framework enables automated differentiation among multiple HCA subtypes while demonstrating strong cross-cohort generalisability for patient-control classification using independent cohorts and rigorous cross-validation when external datasets were unavailable. After age matching wherever required in the differential diagnosis models to address this key confounder, clinical severity was comparable across cohorts, making severity based confounding unlikely (Supplementary Table S3). The robustness of these findings supports the stability and real world potential of eigenmode based biomarkers. This structure based approach also offers a foundation for broader subtype applications and improved accuracy through integration of additional feature maps, methodological refinements, and larger, more heterogeneous training cohorts, particularly for challenging subtype distinctions.

Beyond diagnosis, we addressed another gap: predicting functional features from sMRI alone. A direct comparison with prior work was not possible, as only one previous study[31] suggested that sMRI may be the most informative modality for predicting task-fMRI activation in healthy individuals using DL; however, it did not report any quantitative individual- or population-level prediction accuracy and has not been evaluated in disease cohorts. To our knowledge, this study represents the first demonstration of the feasibility of predicting fMRI equivalent features, leading to reliable approximation of individual activation maps from sMRI alone in both HCs and disease cohorts. Using 5-fold cross-validation, a rigorous approach for modest sample sizes, we achieved moderate-to-strong predictive performance (up to $R^2 \approx 0.6$, correlation ≈ 0.8 for top modes) (Supplementary Table S13). Unlike prior eigenmode-based work reporting >80% reconstruction accuracy for the task activation map at the population level,[34] our estimates reflect individual-level reconstruction, explaining part of the performance gap. Findings in healthy participants were consistent with prior evidence that low-order eigenmodes dominate functional organisation[48] and top predicted modes (Supplementary Table S13) confirmed preserved structure–function mapping across scales, with some disruption of low–frequency mapping in the right hemisphere. The utility of structure-predicted functional features is further detailed in Supplementary Discussion 1. Additioally, hemisphere-specific eigenmode sensitivity to disease progression, eigenmode uniqueness, and the potential for individual-specific brain fingerprinting are further discussed in the Supplementary Discussion 2 and 3.

Finally, although the structure–to–function prediction framework shows promise, several limitations remain. Selecting input features by linear correlation may oversimplify complex dependencies, and training independent models for each functional mode ignores inter-mode relationships. Future work should explore multivariate-input or multi-output architectures including graph–based or surface–based neural networks and examine additional geometric features and multimodal MRI to enhance sensitivity while balancing complexity. Improved anatomical mapping and external validation using datasets with ground–truth fMRI will further strengthen interpretability. A striking aspect of this study is achieving

effective biomarkers for diagnosis and progression in FRDA using only the cerebral cortical analysis, despite the disease primarily affecting the cerebellum. However, this finding is consistent with prior passive movement fMRI studies reporting reduced somatosensory cortical activation in FRDA[36] and with evidence of altered somatomotor, limbic, and visual network involvement.[3] Broadly across HCAs, previous studies reported cortical involvement at varying degrees: reduced gyrification in sensorimotor regions in FRDA,[49] cortical grey matter loss in temporal regions in SCA1,[19] and widespread cortical and subcortical atrophy in SCA3,[50,51] likely contributing to the high diagnostic accuracy observed and the spatial dominance of specific networks in our differential classification models. Progression sensitive functional modes also align with prior reports of evolving cortical activation patterns, although direct comparison is limited given different fMRI paradigms used.[3] Nonetheless, future work integrating both cortical and cerebellar eigenmodes will be critical for brain-wide biomarkers and improved classification in challenging subtypes.

Conclusion

Cortical geometric signatures pave the way for clinically deployable neuroimaging based decision support tools that guide targeted genetic testing, reduce diagnostic delay, and provide objective, scalable, and sensitive biomarkers of disease progression, with important implications for trial design and therapeutic monitoring. Inferring functional signatures from sMRI provides practical fMRI equivalent biomarkers for assessing network disruption and tracking disease progression in movement disorder populations. Overall, our findings highlight a key insight that pathology and cortical architecture may co evolve, with geometric changes shaping structural and functional organisation across HCA progression.

Acknowledgements

The authors gratefully acknowledge the Friedreich's Ataxia Research Alliance (FARA, USA) for funding this project through the Award for Innovative Mindset Grant Scheme (2024).

Full list of TRACK-FA Neuroimaging Consortium members: Professor Nellie GeorgiouKaristianis, Professor Louise A. Corben, Professor Eric F. Lock, Dr Helena Bujalka, Dr Isaac Adanyeguh, Dr Jonathan J. Cherry, Dr Manuela Corti, Professor Martin Delatycki, Dr Imis Dogan, Ms Jennifer Farmer, Professor Marcondes França, Dr Anthony S. Gabay, Professor William Gaetz, Professor Ian H. Harding, Professor Pierre-Gilles Henry, Dr James Joers, Ms Michelle A. Lax, Professor Christophe Lenglet, Mr Jiakun Li, Professor David Lynch, Dr Thomas Mareci, Professor Alberto R. M. Martinez, Professor Massimo Pandolfo, Dr Marina Papoutsi, Dr Richard G. Parker, Dr Myriam Rai, Professor Kathrin Reetz, Dr Thiago J. R. Rezende, Professor Timothy P. Roberts, Dr Sandro Romanzetti, Dr David A. Rudko, Dr Susmita Saha, Professor Jörg B. Schulz, Dr S. H. Subramony, Dr Veena G. Supramaniam.

The authors thank the research coordinators across all TRACK-FA sites for their assistance in participant recruitment and testing.

This work was supported by the MASSIVE HPC facility (www.massive.org.au).

Data sharing statement

Data are available upon reasonable request. Deidentified participant data underlying main results may be provided to researchers who contact the principal investigator of the respective dataset to establish a data-sharing agreement. Approval for data access will be granted on a case-by-case basis at the discretion of the principal investigator.

References

1. Rummey, C. *et al.* Natural History of Friedreich Ataxia: Heterogeneity of Neurologic Progression and Consequences for Clinical Trial Design. *Neurology* **99**, e1499–e1510 (2022).
2. Indelicato, E. *et al.* A global perspective on research advances and future challenges in Friedreich ataxia. *Nature Reviews Neurology* 1–12 (2025).
3. Vavla, M. *et al.* Functional MRI studies in Friedreich's Ataxia: a systematic review. *Frontiers in Neurology* **12**, 802496 (2022).
4. Pandolfo, M. Friedreich ataxia: the clinical picture. *J Neurol* **256 Suppl 1**, 3–8 (2009).
5. National Strategic Action Plan for Rare Diseases 2020. (2020).
6. Zurynski, Y. *et al.* Australian children living with rare diseases: experiences of diagnosis and perceived consequences of diagnostic delays. *Orphanet journal of rare diseases* **12**, 68 (2017).
7. Yau, W. Y. *et al.* Diagnostic yield and limitations of whole-genome sequencing for hereditary cerebellar ataxia. *Brain Communications* **7**, fcaf188 (2025).
8. Kuo, S.-H. *et al.* Delphi study to elicit expert consensus around decision-making in the treatment of Friedreich ataxia. *Frontiers in Neurology* **16**, 1669059 (2025).
9. Pellerin, D. *et al.* Recent advances in the genetics of ataxias: an update on novel autosomal dominant repeat expansions. *Current neurology and neuroscience reports* **25**, 16 (2025).
10. Klockgether, T., Grobe-Einsler, M. & Faber, J. Biomarkers in Spinocerebellar Ataxias. *The Cerebellum* **24**, 104 (2025).
11. Gavriilaki, M. *et al.* Therapeutic biomarkers in Friedreich's ataxia: a systematic review and meta-analysis. *The Cerebellum* **23**, 1184–1203 (2024).
12. Mishra, R. K. *et al.* At-home wearable-based monitoring predicts clinical measures and biological biomarkers of disease severity in Friedreich's Ataxia. *Communications Medicine* **4**, 217 (2024).
13. Öz, G. *et al.* MR imaging in ataxias: consensus recommendations by the ataxia global initiative working group on MRI biomarkers. *The Cerebellum* **23**, 931–945 (2024).
14. Pilotto, F., Del Bondio, A. & Puccio, H. Hereditary ataxias: from bench to clinic, where do we stand? *Cells* **13**, 319 (2024).

15. Naghipour, S. *et al.* Omaveloxolone for the Treatment of Friedreich Ataxia: Efficacy, Safety, and Future Perspectives. *Movement Disorders* **40**, 226–230 (2025).
16. Jain, P., Badgujar, L., Spoorendonk, J. & Buesch, K. Clinical evidence of interventions assessed in Friedreich ataxia: a systematic review. *Therapeutic Advances in Rare Disease* **3**, 26330040221139872 (2022).
17. Lynch, D. R. *et al.* Safety and efficacy of omaveloxolone in Friedreich ataxia (MOXIe study). *Annals of neurology* **89**, 212–225 (2021).
18. Klockgether, T., Mariotti, C. & Paulson, H. L. Spinocerebellar ataxia. *Nat Rev Dis Primers* **5**, 1–21 (2019).
19. Klaes, A. *et al.* MR imaging in spinocerebellar ataxias: a systematic review. *American Journal of Neuroradiology* **37**, 1405–1412 (2016).
20. Selvadurai, L. P. *et al.* Multiple mechanisms underpin cerebral and cerebellar white matter deficits in Friedreich ataxia: The IMAGE□FRDA study. *Human Brain Mapping* **41**, 1920–1933 (2020).
21. Georgiou□Karistianis, N. *et al.* Neuroimaging Biomarkers for Friedreich Ataxia: A Cross□Sectional Analysis of the TRACK□FA Study. *Annals of Neurology* (2025).
22. Agrawal, S., Agrawal, R. K., Kumaran, S. S., Rana, B. & Srivastava, A. K. Integration of graph network with kernel SVM and logistic regression for identification of biomarkers in SCA12 and its diagnosis. *Cerebral Cortex* **34**, (2024).
23. Tamuli, D. *et al.* Autonomic function based classification of spinocerebellar ataxia type 1 and 2 using machine learning classifiers. *Indian J Physiol Pharmacol* **61**, 323–332 (2017).
24. Yang, Z., Zhong, S., Carass, A., Ying, S. H. & Prince, J. L. Deep learning for cerebellar ataxia classification and functional score regression. in 68–76 (Springer, 2014).
25. Cao, T. *et al.* Are neuroanatomical phenotypes for psychiatric disorders robust? An assessment of the reproducibility of grey matter differences in mental illness. *medRxiv* 2025–07 (2025).

26. Saha, S., Corben, L. A., Selvadurai, L. P., Harding, I. H. & Georgiou-Karistianis, N. Predictive machine learning and multimodal data to develop highly sensitive, composite biomarkers of disease progression in Friedreich ataxia. *Scientific Reports* **15**, 17629 (2025).
27. Rezende, T. J. *et al.* Sensitivity of advanced magnetic resonance imaging to progression over six months in early spinocerebellar ataxia. *Movement Disorders* **39**, 1856–1867 (2024).
28. Kerestes, R. *et al.* Reduced cerebello-cerebral functional connectivity correlates with disease severity and impaired white matter integrity in Friedreich ataxia. *Journal of Neurology* **270**, 2360–2369 (2023).
29. Guo, J. *et al.* Cerebello□cerebral resting□state functional connectivity in spinocerebellar ataxia type 3. *Human Brain Mapping* **44**, 927–936 (2023).
30. Borbely, K. Functional neuroimaging in movement disorders. *Orvosi Hetilap* **142**, 2347–2355 (2001).
31. Ellis, D. G. & Aizenberg, M. R. Structural brain imaging predicts individual-level task activation maps using deep learning. *Frontiers in Neuroimaging* **1**, 834883 (2022).
32. Müller, E. J., Munn, B. R., Aquino, K. M., Shine, J. M. & Robinson, P. A. The music of the hemispheres: Cortical eigenmodes as a physical basis for large-scale brain activity and connectivity patterns. *Frontiers in human neuroscience* **16**, 1062487 (2022).
33. Cao, T. *et al.* Mode□based morphometry: A multiscale approach to mapping human neuroanatomy. *Human Brain Mapping* **45**, e26640 (2024).
34. Pang, J. C. *et al.* Geometric constraints on human brain function. *Nature* 1–9 (2023).
35. Olsen, A. S., Pang, J. C., Zalesky, A., Van De Ville, D. & Behjat, H. On reconstruction of cortical functional maps using subject-specific geometric and connectome eigenmodes. in 1–5 (IEEE, 2025).
36. Destrebecq, V., Rovai, A., Trotta, N., Comet, C. & Naeije, G. Proprioceptive and tactile processing in individuals with Friedreich ataxia: an fMRI study. *Front Neurol* **14**, 1224345 (2023).
37. Georgiou-Karistianis, N. *et al.* A natural history study to track brain and spinal cord changes in individuals with Friedreich's ataxia: TRACK-FA study protocol. *Plos one* **17**, e0269649 (2022).

38. Rezende, T. J. *et al.* Progressive spinal cord degeneration in Friedreich's ataxia: results from ENIGMA ataxia. *Movement disorders* **38**, 45–56 (2023).

39. Rezende, T. J. R. *et al.* Structural signature of SCA3: from presymptomatic to late disease stages. *Annals of neurology* **84**, 401–408 (2018).

40. Martins Junior, C. R. *et al.* Structural signature in SCA1: clinical correlates, determinants and natural history. *Journal of Neurology* **265**, 2949–2959 (2018).

41. Goscinski, W. J. *et al.* The multi-modal Australian ScienceS Imaging and Visualization Environment (MASSIVE) high performance computing infrastructure: applications in neuroscience and neuroinformatics research. *Frontiers in Neuroinformatics* **8**, 30 (2014).

42. Chen, Y.-C. *et al.* The individuality of shape asymmetries of the human cerebral cortex. *Elife* **11**, e75056 (2022).

43. Yeo, B. T. *et al.* The organization of the human cerebral cortex estimated by intrinsic functional connectivity. *Journal of neurophysiology* (2011).

44. Meira, A. T. *et al.* Neuroimaging in Cerebellar Ataxias: A Diagnostic Approach. *The Cerebellum* **24**, 154 (2025).

45. Scaravilli, A. *et al.* CHARON: an imaging-based diagnostic algorithm to navigate through the sea of hereditary degenerative ataxias. *The Cerebellum* **23**, 2122–2129 (2024).

46. Tamuli, D. *et al.* Cortical and subcortical brain area atrophy in SCA1 and SCA2 patients in India: the structural MRI underpinnings and correlative insight among the atrophy and disease attributes. *Neurology India* **69**, 1318–1325 (2021).

47. Hu, J. *et al.* Pattern of cerebellar grey matter loss associated with ataxia severity in spinocerebellar ataxias type 3: a multi-voxel pattern analysis. *Brain Imaging and Behavior* **16**, 379–388 (2022).

48. Huo, S. & Liu, Z. Condensation of eigenmodes in functional brain network and its correlation to chimera state. *Communications Physics* **6**, 285 (2023).

49. Selvadurai, L. P. *et al.* Longitudinal structural brain changes in Friedreich ataxia depend on disease severity: the IMAGE-FRDA study. *Journal of Neurology* **268**, 4178–4189 (2021).

50. De Rezende, T. *et al*. Cerebral cortex involvement in Machado− Joseph disease. *European journal of neurology* **22**, 277-e24 (2015).

51. Wan, N., Chen, Z., Wan, L., Tang, B. & Jiang, H. MR imaging of sca3/mjd. *Frontiers in neuroscience* **14**, 749 (2020).